

Oxide semiconductors find a large application as chemical sensors for process control and environmental monitoring. Apart from the kinetics of chemical interaction between the analyte and the semiconductor which leads to electron transfer across the gas-solid interface, carrier concentration in the conduction/valence bands, band gap, dopants, stability of the compound in the operating environment, temperature, etc. will decide the choice of the semiconducting oxide for a given application. The selectivity of a given oxide towards a specific analyte in the presence of various other analyte species is determined mainly by the relative chemical interaction of the chosen oxide material towards specific analyte and the temperature dependent kinetics of the interaction which leads to judicious choice of the operating temperature. Different oxygen species are proposed to be involved during the sensing process, namely chemisorbed oxygen species (O^- , O_2^- , etc.) which control the surface carrier concentration or the lattice oxygen (oxide ion vacancy). Sensitivity, on the other hand, can be improved by using the particles of high specific surface area to maximize the probability of chemical interaction. This is accomplished in thin film configuration or thick film composed of nanocrystalline powders of the oxide.

In this presentation, three different types of oxides are chosen, viz. a) sensing action mediated by conventionally encountered, chemisorbed oxygen species, b) sensing by both chemisorbed and lattice oxygen species and c) predominant involvement of lattice oxygen alone in sensing. For this purpose, trace level sensing of hydrogen in argon using tin oxide, trace to a few thousands ppm level sensing of hydrogen in argon by chromium niobate and trace level sensing of ammonia by silverdecamolybdate were chosen as examples, for the three types of sensing processes. The details of the experiments and the observations made will be presented in this paper.

Hydrothermal synthesis and electrochemical properties of $Fe_{1.19}(PO_4)(OH)_{0.57}(H_2O)_{0.43}/C$ cathode material for Li-ion batteries

Abdelfattah Mahmoud^{*1}, Claude Karegeya¹, Moulay Tahar Sougrati³, Bénédicte Vertruyen¹, Rudi Cloots¹, Pierre-Emmanuel Lippens³, Frédéric Boschini¹

¹GREENMAT, CESAM, Institute of Chemistry B6, University of Liège, 4000 Liège, Belgium

³Institut Charles Gerhardt, UMR 5253 CNRS, Université de Montpellier, France

Email: abdelfattah.mahmoud@uliege.be

Abstract

Recent rapid development of the portable electronic devices, growing interest in the electric vehicles and increasing integration the renewable energies required the development of cost-effective and high energy storage systems. Lithium-ion batteries are considered as system of the choice for variety of mobile and stationary applications. However, new electrode materials are demanded to increase the energy density of Li-ion batteries.

This presentation will report on the preparation and study of $Fe_{1.19}(PO_4)(OH)_{0.57}(H_2O)_{0.43}/C$ (FPHH/C) composite as positive electrode material with high capacity and long cycle-life [1, 2]. FPHH/C (C= carbon black (CB) and carbon nanotubes (CNT)) composites were obtained by one-step the hydrothermal synthesis route. These cathode materials showed an excellent reversible capacity corresponding to 1.19 Li reaction. This is attributed to the stable and open structure of FPHH and also to the effect of carbon addition (CB and CNT) that improves the electronic percolation of the composite. The study of the reaction mechanism of FPHH/CNT during cycling by combining operando XRD and ^{57}Fe Mossbauer spectroscopy (**Figure 1**) shows that the insertion mechanism is a monophasic reaction with 10% volume variations associated to the Fe^{3+}/Fe^{2+} redox reaction [2].

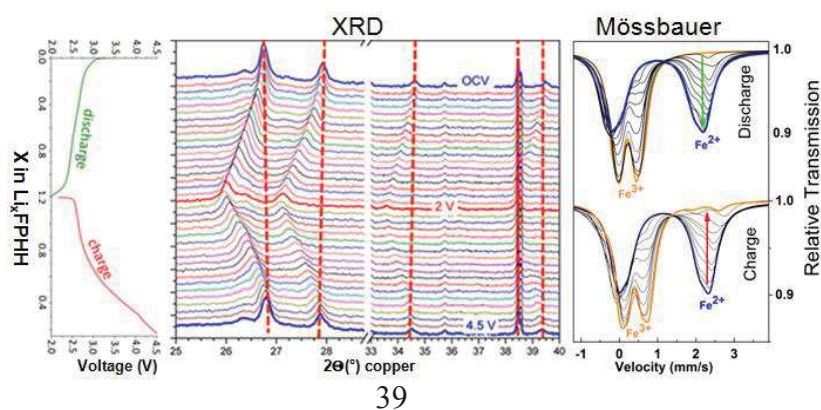


Figure 1. Voltage curve (left), operando XRD patterns (middle) and operando ^{57}Fe Mössbauer spectra (right) of FPHH/CNT for the first discharge–charge cycle at C/20.

References

1. C. Karegeya, A. Mahmoud, R. Cloots, B. Vertruyen, F. Boschini. *Electrochimica Acta* 250 (2017) 49-58.
2. A. Mahmoud, C. Karegeya, M. T. Sougrati, J. Bodart, B. Vertruyen, R. Cloots, P-E. Lippens, F. Boschini. *ACS Applied Materials and interfaces* 10 (2018) 34202-34211.

Ionic Liquid Based Thermo-electrochemical Cell for Power Generation

Mohd Faizul Mohd Sabri, Syed Waqar Hasan, Suhana Mohd Said, Nur Awanis Hashim, Mohd Faiz Mohd Salleh

Faculty of Engineering, University of Malaya, 50603 Kuala Lumpur, Malaysia

Abstract

Thermo-Electrochemical cells (Thermocells/TECs) convert thermal energy into electricity by means of electrochemical potential disequilibrium between electrodes induced by a temperature gradient (ΔT). Thus, the ΔT is an important parameter in determining the conversion efficiency. In this work, Poly(Vinylidene Fluoride) (PVDF) membrane is introduced in thermocells to mitigate the heat transfer effects in order to maintain high ΔT . Experimental results shows that at a ΔT of 12 K, an improvement in the open circuit voltage (V_{oc}) of the TEC from 1.3 mV to 2.8 mV is obtained by employment of the membrane. The PVDF membrane is employed at three different locations between the electrodes i.e. $x=2$ mm, 5 mm, and 8 mm where 'x' defines the distance between the cathode and PVDF membrane. We found that the membrane position at $x=5$ mm achieves the closest internal ΔT (i.e. 8.8 K) to the externally applied ΔT of 10 K and corresponding power density is 254 nWcm⁻²; 78% higher than the conventional TEC. Finally, a thermal resistivity model based on infrared thermography explains mass and heat transfer within the thermocells.

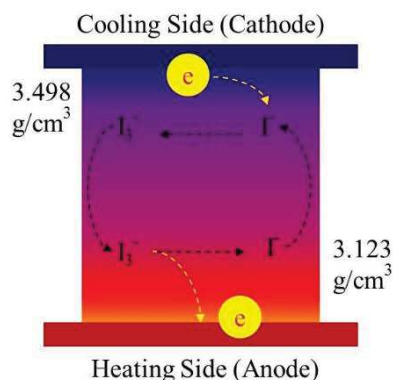


Fig.1. Cell configuration of Thermo-Electrochemical Cell

References

1. Hasan SW, Said SM, Sabri MFM, Bakar ASA, Hashim NA, Hasnan MMIM, Pringle JM, MacFarlane DR, *Sci Rep* (2016) 6:1–11
2. SW Hasan, SM Said, MFM Sabri, HA Jaffery, ASBA Bakar, *Macromol. Mater. Eng.* (2018), 303, 3
3. Snyder GJ, Toberer ES, *Nat Mater* (2008) 7:105–114
4. Mohanraman R, Lan T-W, Hsiung T-C, Amada D, Lee P-C, Ou M-N, Chen Y-Y, *Front Chem* (2015) 3:63